2017 SCEC Project Report * Project 17065
Estimating seismic coupling in southern California using aftershock productivity and geodetic constraints

1. PROJECT GOALS

The goals of the project are to (i) *estimate the seismic coupling in southern California using the connection between seismic coupling and aftershock productivity suggested by the damage rheology modeling,* and (ii) *obtain additional constraints on the seismic coupling estimation using geodetic modeling.*

2. PROJECT METHODOLOGY

We briefly summarize below the methodological background of the project and the main challenges of the respective data analysis.

2.1 Estimating seismic coupling using aftershock productivity

The seismic coupling χ is defined as the fraction of the stored elastic strain energy that is released by brittle deformation (i.e. earthquakes). Damage rheology modeling of *Ben-Zion and Lyakhovsky* [2006] suggests that the seismic coupling coefficient χ can be estimated using aftershock productivity K, defined as the total number of direct aftershocks produced by a mainshock. *Zaliapin and Ben-Zion* [2013a,b] showed that the average number of aftershocks for a mainshock of magnitude m is independent of m when aftershocks are collected within a fixed magnitude range [m-Δ, m]; this approach is referred to as Δ-analysis. This implies, in particular, that

$$K = K_0 10^{\lambda\Delta}. \tag{1}$$

Eq. (2) allows one using numerous aftershock series of small-to-medium-magnitude events with a fixed value of Δ to improve the regional estimation of K_0. For two sub-regions indexed by i = 1,2 one can relate the respective seismic couplings via the coefficient $\kappa := K_{01}/K_{02}$

$$\chi_2 \approx \frac{1}{\kappa\left(1/\chi_1 - 1\right) + 1}. \tag{2}$$

Equation (3) can be used to evaluate the seismic coupling χ_2 in a given region from knowledge of seismic coupling χ_1 in a reference (well-instrumented and well-studied) region. The only needed parameter is κ that can be efficiently estimated using aftershocks stacking.

2.2 Geodetic constraints on seismic coupling

Geodetic information complements the approach described in **Sect. 1.1** in constraining the seismic coupling. The geodetic approach fits the available GPS velocity observations (typical duration 2-20 years) to infer a model of the geodetic deformation field; this model is then used to predict the corresponding moment rate $\dot{M}_{\text{geodetic}}$. Given the plate-boundary-wide agreement between geodetic and geologic deformation rates, one can consider geodetic estimations of the moment rate to correspond to the long-term kinematics. The regional seismic coupling χ is related to the ratio C between the observed seismic moment M_{seismic} and predicted geodetic moment M_{geodetic}:

$$C(A,T) = \frac{M_{\text{seismic}}}{M_{\text{geodetic}}} = \frac{\sum_i M_i}{T\dot{M}_{\text{geodetic}}}, \tag{3}$$

where the summation in the numerator is taken for the seismic moments M_i [Nm] of all events within a region of area A [km^2] and time duration T [yrs]. Ideally, as the area A and time T increase, the ratio C approaches the seismic coupling χ. In this project, we calculate the geodetic moment from different strain rate models. Importantly, we use v.2.1 of the Global Strain Rate Model (GSRM) [*Kreemer et al.,* 2014] which is a high-resolution spatially continuous model based on a spline interpolation technique in which model velocities are fitted to observed GPS velocities in a least-squares sense, using the full data covariance matrix. Velocities are then interpolated to derive a continuous velocity gradient tensor field. This approach was also used in a high-resolution regional western U.S. study [*Kreemer et al.*, 2012]. The other strain rate model we propose to apply uses SCEC's CGM velocity field and a new strain rate determination algorithm that uses robust statistics to estimate the strain rate field [*Kreemer et al.*, 2017]. The algorithm is called MELD: Median Estimation of Local Deformation.

3. RESULTS

Here we summarize the project results, as well as methodologic developments that address several challenges in a practical implementation of the coupling estimation of **Sects. 2.1, 2.2**. One category of challenges arises from the realization that multiple elements of the coupling analysis (cluster productivity, seismic moment release, strain rates) are not stationary in time, with significant variations that affect a naïve estimation. Another category refers to the existence of different types of earthquake clusters with distinct productivity properties – the existence of different cluster types must be taken into account when estimating cluster productivity.

3.1 Estimating seismic coupling

An example of seismic coupling estimation according to the methodology of Sect. 2.1 is shown in Fig. 1. Here we use average branching in clusters with magnitude $m > 4$ as a proxy for earthquake productivity K. This result is in agreement with the known properties of seismic coupling in California – the coupling is generally lower in high heat flow regions (Coso, Salton Sea) and is higher in cold regions (Mojave, Ventura). The stability of this result with respect to various components of the analysis is to be explored within the remaining duration of the project.

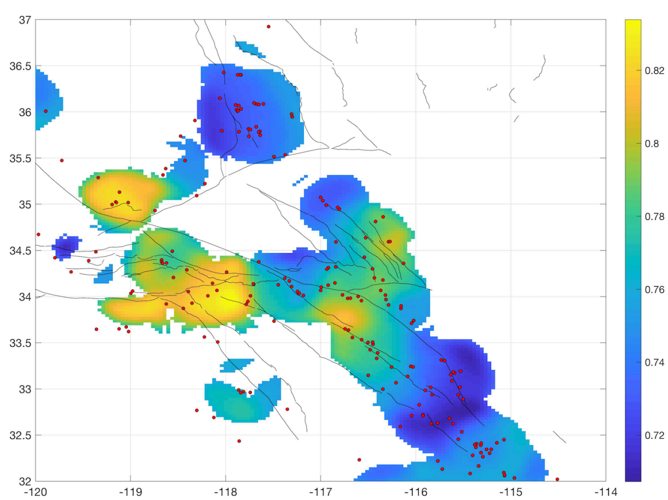

Figure 1: Estimating seismic coupling coefficient in southern California using earthquake productivity: an example. Color code corresponds to the values of coupling. Black lines show the main faults, Red dots show epicenters of earthquakes with $m > 4$ used for analysis.

3.2 Cluster identification and catalog declustering

Identification of earthquake clusters (and aftershocks in particular), necessary for estimating K_0. This analysis is affected by space-time varying earthquake location quality and catalog completeness. Traditionally, the estimation of K is done by using only the aftershock sequences of the largest earthquakes, which may lead to various biases, as documented in *Zaliapin and Ben-Zion* [2013b].

We developed an improved methodology for catalog declustering and cluster identification. The focus was on treatment of the large events. The spatio-temporal extent of the aftershock sequences of such events is substantially overlapping with that of the background, which triggers cluster identification errors (misidentified background and/or cluster events). To resolve this problem, we developed an algorithm that only uses space-time characteristics of events, not their magnitudes. This has shown to produce more accurate cluster identification and substantially reduce the identification errors of both types. Specifically, we apply a nearest-neighbor technique in time-space-magnitude domain to separate observed earthquakes into an independent population of background events (likely produced directly by tectonic and other loadings) and a dependent population clustered around (and likely triggered by) the background events. The proposed declustering method differs from existing techniques by (i) simple parameterization (only 3 readily estimated parameters), (ii) weak sensitivity to parameter values and catalog uncertainties, (iii) absence of ad-hoc assumptions about a cluster model. The technique is applied to a variety of catalogs and the declustering quality is assessed using several space-time or temporal tests of homogeneity. The new declustering algorithm can facilitate a range of studies, targeted at both earthquake cluster properties and properties of the background flow of events.

3.2 Temporal variations of the observed seismic moment release

Stationarity of seismic moment release, on suitable time scales (say, tens of years), is among the main assumptions used in evaluating seismic coupling by geodetic methods, as discussed in **Sect. 2.1.** Violations of this assumptions may lead to biased estimations. As Eq. (4) implies, the coupling coefficient will be overestimated during the periods of increased moment release and it will be underestimated during period of decreased moment release.

We demonstrated that the observed seismic moment does vary on time scales of tens of years in a global catalog (**Fig. 2**). Specifically, we revisited the significance of the increased number of great earthquakes since 2005. The global rate of great earthquakes exhibits an increase since 2005. The question of whether this increase is an expected statistical variation of a time-independent process or an evidence of genuine temporal fluctuations has received substantial attention. A conventional way of addressing this problem is to consider the number of events above a threshold, and to test possible deviations from a stationary Poisson process. We argue that this approach might not be powerful enough. Instead, to reveal if the observed change is a significant deviation from a long-term expectation, it is important to (i) analyze moment release, not only the number of events, (ii) consider large enough range of examined moments – say, all events with magnitude above Mw = 7, and (iii) consider sequential moment release, not the statistical distribution of all moments collected during the examined time interval. Our analysis combines these aspects and indicates that, at variance with the majority of studies referenced above, a time-independent model cannot describe the global moment release. In particular, the apparent increase of moment release during the last decade is a statistically significant feature of the global seismic process. Analysis of the global moment release during 1918–2014 inferred from the International Seismological Centre (ISC) catalog rejects a null hypothesis of independence between earthquake seismic moments and occurrence times. Our results suggest the existence of temporal variation in the seismic moment distribution on a global scale with decreased moment release during 1975–2004 and a transition to a regime with increased moment release during the 1960s and after 2004. We use complementary likelihood and regression analyses based on non-parametric resampling and parametric Monte Carlo simulations to construct tests powerful enough to reject the independence null hypothesis.

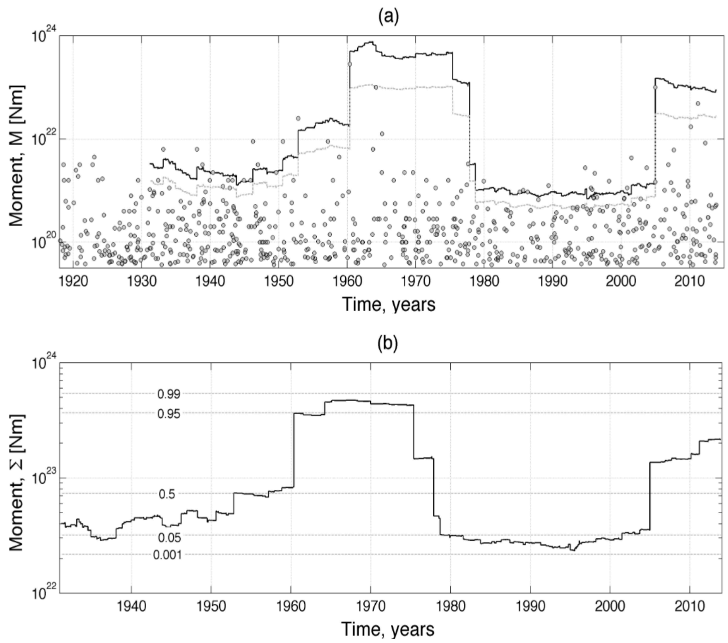

Figure 2: Time fluctuations of the global seismic moment release: an illustration. The analysis uses 692 declustered earthquakes with $M_w \geq 7$ ($M \geq 3.55\times10^{19}$ Nm) during 1918 – 2014 from version 4 of the ISC-GEM catalog. (a) Examined events (gray circles) and the estimated corner moment M_c of tapered Pareto distribution (solid line) as a function of time. The estimation is done in a sliding window of 100 events. A lower 95% confidence boundary is shown by dashed line; the upper limit is unconstrained. (b) The observed moment release $\Sigma_{100}(t)$ in a sliding window of m = 100 events (solid line) vs. empirical quantiles (dashed lines) obtained using 10^5 resamplings of the observed moments. The level of quantiles in indicated in the figure. After *Zaliapin and Kreemer*, 2017.

3.3 Seasonal variations of strain rates

One of the most intriguing observations made during the geodetic modeling of the Western US is the existence of prominent seasonal (annual) variations of the dilatation strain rate, within $\pm$ 4×10^{-9} yr^{-1} illustrated in Fig. 3. The results are obtained by applying MELD to the modeled seasonal variation from horizontal GPS time-series. Note how the seasonal pattern predicts opposing pattern for Southern and Northern California.

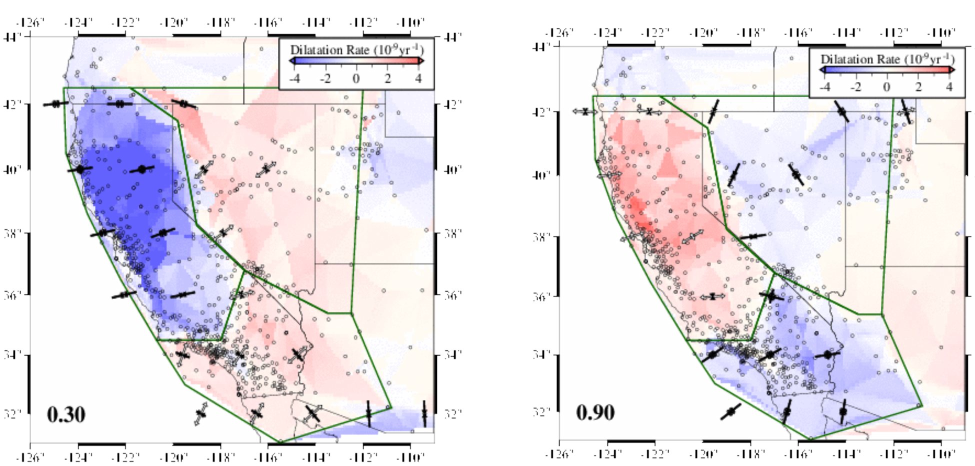

Figure 3: Colors reflect the dilatational component of the horizontal seasonal variations of the strain rate in California – Great Basin area (blue is contraction, red is extension). Vectors are principal strain orientations. Left panel: time 0.3 of the annual cycle (April). Right panel: time 0.9 of the annual cycle (November). Green polygons outline focus areas examined in Fig. 4.

3.4 Annual fluctuations of the earthquake clustering

Importantly, the detected that fluctuations of the strain rate match well fluctuations of earthquake cluster parameters. We considered the relocated catalog of *Hauksson et al.* [2013] in southern California during Jan. 1981 – Dec. 2013 with minimum magnitude m = 2. The catalog contains 117,076 events. The analysis is performed within the strain-rate polygons outlined in Fig. 3 that coarsely correspond to southern and northern California. We also used the catalog of *Waldhauser and Schaff* [2008] that covers northern California. We found that multiple properties of earthquale clusters demonstrate seasonal variations well aligned with the fluctuations of the strain rates.

3.4 Different types of earthquake clusters

3.4.1 Earthquake clustering in relation to hydraulic activities at geothermal fields in California

Martinez-Garzon et al. [2018] investigated earthquake cluster properties in relation to fluid balance $H(t)$ (the difference of fluid injection and production rates) using about nine years of data from The Geysers (both the entire field and a local subset), Coso and Salton Sea geothermal fields in California. Individual earthquake clusters are identified and classified using the nearest-neighbor approach of *Zaliapin and Ben-Zion* [2013a, 2013b]. These are used to calculate nine complementary cluster statistics as time series with a step of about one month. Three alternative techniques (moving window correlation, analysis of variance, regression) are employed to assess the relations between (possibly non-stationary) time series of cluster statistics and $H(t)$. A total of 108 pairwise relations between cluster statistics and $H(t)$ are analyzed to clarify effects of fluid activities on seismicity in different places. The seismic clustering response to the fluid balance differs among the examined fields. The Geysers and Salton Sea areas display the highest and lowest clustering responses, respectively. The proportion of clusters consisting of a single event with no offspring (singles) is correlated significantly with $H(t)$ at all examined datasets, with a lower proportion of singles during periods of high fluid balance. This may reflect increased susceptibility to earthquake triggering in time intervals with high injection rates. The background seismicity rates significantly increase with $H(t)$ at the Geysers and Coso, while an opposite relation holds at the Salton Sea. This could be related to the high structural and tectonic complexity at the Salton Sea compared to the other two geothermal fields.

3.4.2 Systematic detection and classification of earthquake clusters in Italy

We performed a systematic analysis of spatio-temporal clustering of 2007-2017 earthquakes in Italy with magnitudes m>3 [*Poli et al.*, 2018]. The study employs the nearest-neighbor approach of *Zaliapin and Ben-Zion* [2013a, 2013b] with basic data-driven parameters. The results indicate that seismicity in Italy (an extensional tectonic regime) is dominated by clustered events, with smaller proportion of background events than in California. Evaluation of internal cluster properties allows separation of swarm-like from burst-like seismicity. This classification highlights a strong geographical coherence of cluster properties. Swarm-like seismicity are dominant in regions characterized by relatively slow deformation with possible elevated temperature and/or fluids (e.g. Alto Tiberina, Pollino), while burst-like seismicity is observed in crystalline tectonic regions (Alps and Calabrian Arc) and in Central Italy where moderate to large earthquakes are frequent (e.g. L'Aquila, Amatrice). To better assess the variation of seismicity style across Italy, we also perform a clustering analysis with region-specific parameters. This analysis highlights clear spatial changes of the threshold separating background and clustered seismicity and permits better resolution of different clusters in specific geological regions. For example, a large proportion of repeaters is found in the Etna region as expected for volcanic-induced seismicity. A similar behavior is observed in the northern Apennines with high pore pressure associated with mantle degassing. The observed variations of earthquakes properties highlight shortcomings of practices using large-scale average seismic properties, and points to connections between seismicity and local properties of the lithosphere. The observations help to improve the understanding of the physics governing the occurrence of earthquakes in different regions.

References

Ben-Zion, Y. (2008) Collective behavior of earthquakes and faults: continuum-discrete transitions, progressive evolutionary changes and different dynamic regimes, Rev. Geophys., 46, RG4006, doi:10.1029/2008RG000260.

Ben-Zion, Y. and V. Lyakhovsky (2002). Accelerated Seismic Release and Related Aspects of Seismicity Patterns on Earthquake Faults, *Pure Appl. Geophys*., **159**, 2385–2412.

Ben-Zion, Y. & Lyakhovsky, V. (2006). Analysis of aftershocks in a lithospheric model with seismogenic zone governed by damage rheology, *Geophys. J. Int.*, 165, 197–210.

Hauksson, E., W. Yang, and P. M. Shearer (2012) Waveform Relocated Earthquake Catalog for Southern California (1981 to June 2011); Bull. Seismol. Soc. Am., 102, 5, 2239-2244. doi: 10.1785/0120120010.

Hauksson, E., W. Yang, and P. M. Shearer (2013), Waveform Relocated Earthquake Catalog for Southern California, 1981-2013; available from http://www.data.scec.org/research-tools/downloads.html

Kreemer, C., Hammond, W.C., Blewitt, G., Austin, A.A., and Bennett, R.A. (2012) A geodetic strain rate model for the Pacific-North American plate boundary, western United States**,** *Nevada Bureau of Mines and Geology Map 178*, scale 1:1,500,000.

Kreemer, C., Holt, W.E., and Haines, A.J. (2002) The global moment rate distribution within plate boundary zones**,** in *Plate Boundary Zones, Geodynamics Series*, eds. S. Stein, and J.T. Freymueller, v. 30, p. 173–190, doi:10/1029/030GD10, AGU, Washington, D.C., 2002.

Kreemer, C., G. Blewitt, and E. C. Klein (2014), A geodetic plate motion and Global Strain Rate Model, *Geochem. Geophys. Geosystems*, 15(10), 3849–3889, doi:10.1002/2014GC005407.

Kreemer, C., Hammond, W.C., and G. Blewitt (2017), A robust estimation of the 3D intraplate deformation of the North American plate from GPS, Journal of Geophysical Research https://doi.org/10.1029/2017JB015257

Martínez-Garzón, P., I. Zaliapin, Y. Ben-Zion, G. Kwiatek and M. Bohnhoff (2018) Comparative study of earthquake clustering in relation to hydraulic activities at geothermal fields in California, *J. Geophys. Res.*, doi: 10.1029/2017JB014972

Waldhauser, F. and D.P. Schaff (2008) Large-scale relocation of two decades of Northern California seismicity using cross-correlation and double-difference methods, *J. Geophys. Res*., 113, B08311, doi:10.1029/2007JB005479.

Zaliapin, I. and Y. Ben-Zion (2013a) Earthquake clusters in southern California, I: Identification and stability. J. Geophys. Res., 118, 2847-2864.

Zaliapin, I. and Y. Ben-Zion (2013b) Earthquake clusters in southern California, II: Classification and relation to physical properties of lithosphere. *J. Geophys. Res*., 118, 2865-2877.

Zaliapin, I. and C. Kreemer (2017) Systematic fluctuations in the global seismic moment release. *Geophys. Res. Lett.,* 44, 4820-–4828, doi:10.1002/2017GL073504

Project publications

Papers

1. Martínez-Garzón, P., I. Zaliapin, Y. Ben-Zion, G. Kwiatek and M. Bohnhoff (2018) Comparative study of earthquake clustering in relation to hydraulic activities at geothermal fields in California, *J. Geophys. Res.*, doi: 10.1029/2017JB014972
2. Zaliapin, I. and C. Kreemer (2017) Systematic fluctuations in the global seismic moment release. *Geophys. Res. Lett.,* 44, 4820—4828, doi:10.1002/2017GL073504

Conference abstracts

1. Martínez-Garzón, P., I. Zaliapin, Y. Ben-Zion, G. Kwiatek and M. Bohnhoff (2018) Comparative study of earthquake clustering in relation to hydraulic activities at geothermal fields in California. A poster presented at *2018 Annual Meeting of Seismological Society of America,* May 14-17, Miami, FL

2. Poli, P., Y. Ben-Zion, and I. Zaliapin (2017) Systematic detection and classification of earthquake clusters in Italy. Abstract S21B-0707 presented at *2018 Fall Meeting of AGU, New Orleans*, December 11-15, 2017.

3. Martínez-Garzón, P., I. Zaliapin, Y. Ben-Zion, G. Kwiatek and M. Bohnhoff (2017) Comparative study of earthquake clustering in relation to hydraulic activities at geothermal fields in California, Abstract S12A-02 presented at *2018 Fall Meeting of AGU, New Orleans*, December 11-15, 2017.

4. Zaliapin, I. and Y. Ben-Zion (2017) Quantifying the coalescence process of microcracks leading to a system-size failure. *Proc. of Southern California Earthquake Center (SCEC) 2017 Annual Meeting*, Palm Springs, CA, September 10-13, 2017, Vol. XXVII, poster 187.

5. Kraner, M., W. Hammond, C. Kreemer, and I. Zaliapin (2017) Seasonal Variation of Strain in Central California and its Correlation with Seismicity. *Proc. of Southern California Earthquake Center (SCEC) 2017 Annual Meeting*, Palm Springs, CA, September 10-13, 2017, Vol. XXVII, poster 212.

Papers in preparation

1. Poli, P., Y. Ben-Zion and I. Zaliapin (2018) Systematic detection and classification of earthquake clusters in Italy.

2. Zaliapin, I. and Y. Ben-Zion (2018) Earthquake declustering via nearest-neighbor approach in time-space-magnitude domain.